Science Advances
AAAS

Supplementary Materials for

Iron oxide nanoparticles augment the intercellular mitochondrial transfer–mediated therapy

Ting Huang, Tianyuan Zhang*, Xinchi Jiang, Ai Li, Yuanqin Su, Qiong Bian, Honghui Wu, Ruyi Lin, Ni Li, Hongcui Cao, Daishun Ling, Jinqiang Wang, Yasuhiko Tabata, Zhen Gu*, Jianqing Gao*

*Corresponding author. Email: tianyuanzhang@zju.edu.cn (T.Z.); guzhen@zju.edu.cn (Z.G.); gaojianqing@zju.edu.cn (J.G.)

Published 29 September 2021, *Sci. Adv.* **7**, eabj0534 (2021)
DOI: 10.1126/sciadv.abj0534

The PDF file includes:

Figs. S1 to S30
Legends for movies S1 and S2

Other Supplementary Material for this manuscript includes the following:

Movies S1 and S2

Supplementary Figures

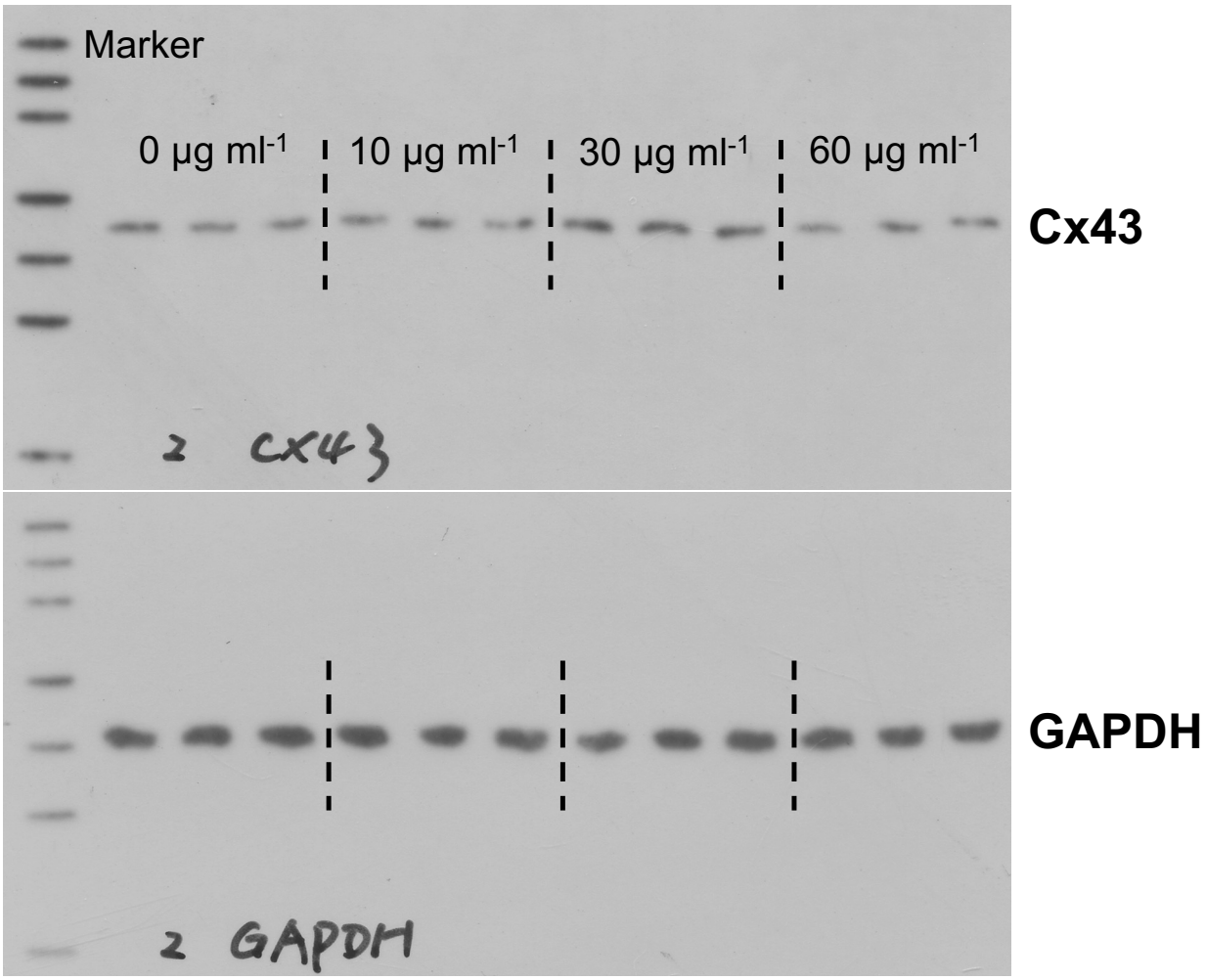

Fig. S1. Iron oxide nanoparticles (IONPs) triggered the connexin 43 (Cx43) overexpression of hMSC. Western blot analysis was applied to assess the Cx43 expressions of hMSCs after the cellular uptake of IONPs at diverse concentrations. Each group was repeated for thrice (n = 3). GAPDH: glyceraldehyde-3-phosphate dehydrogenase.

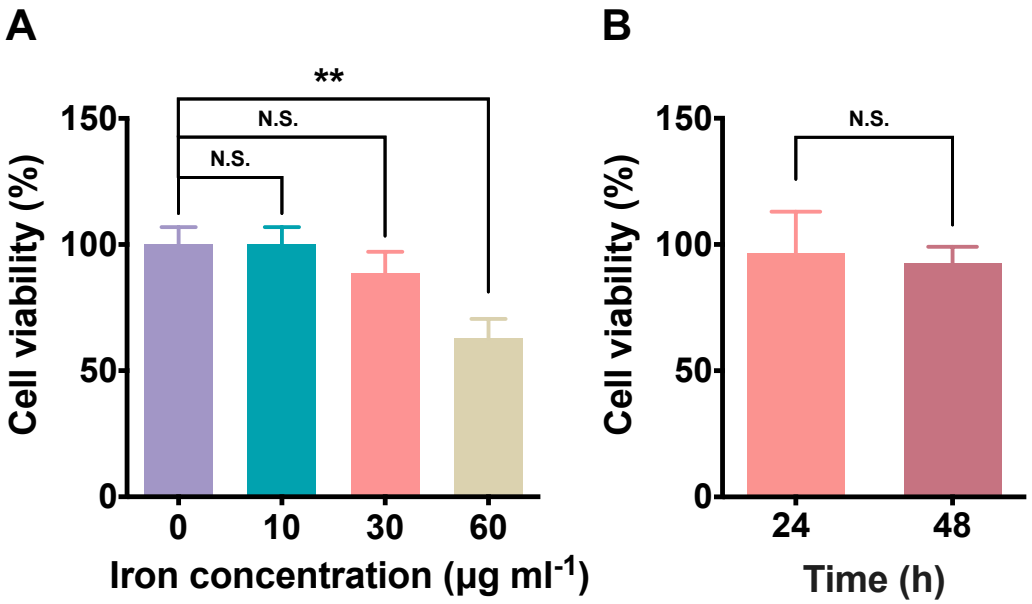

Fig. S2. Cell viability of hMSCs post the cellular uptake of IONPs assessed via CCK-8 kit. (A) Cell viability of hMSCs at 24 h post the treatment of IONPs with different concentrations (n = 3). **(B)** Cell viability of hMSCs at 24 h and 48 h after the treatment of IONPs with the concentration of 30 μg ml^{-1} (n = 3). Data are presented as means ± SD. Statistical significance was calculated via ordinary one-way analysis of variance (ANOVA) (A) and unpaired Student's t test (B). $^{**}P < 0.01$, N.S., no significant difference.

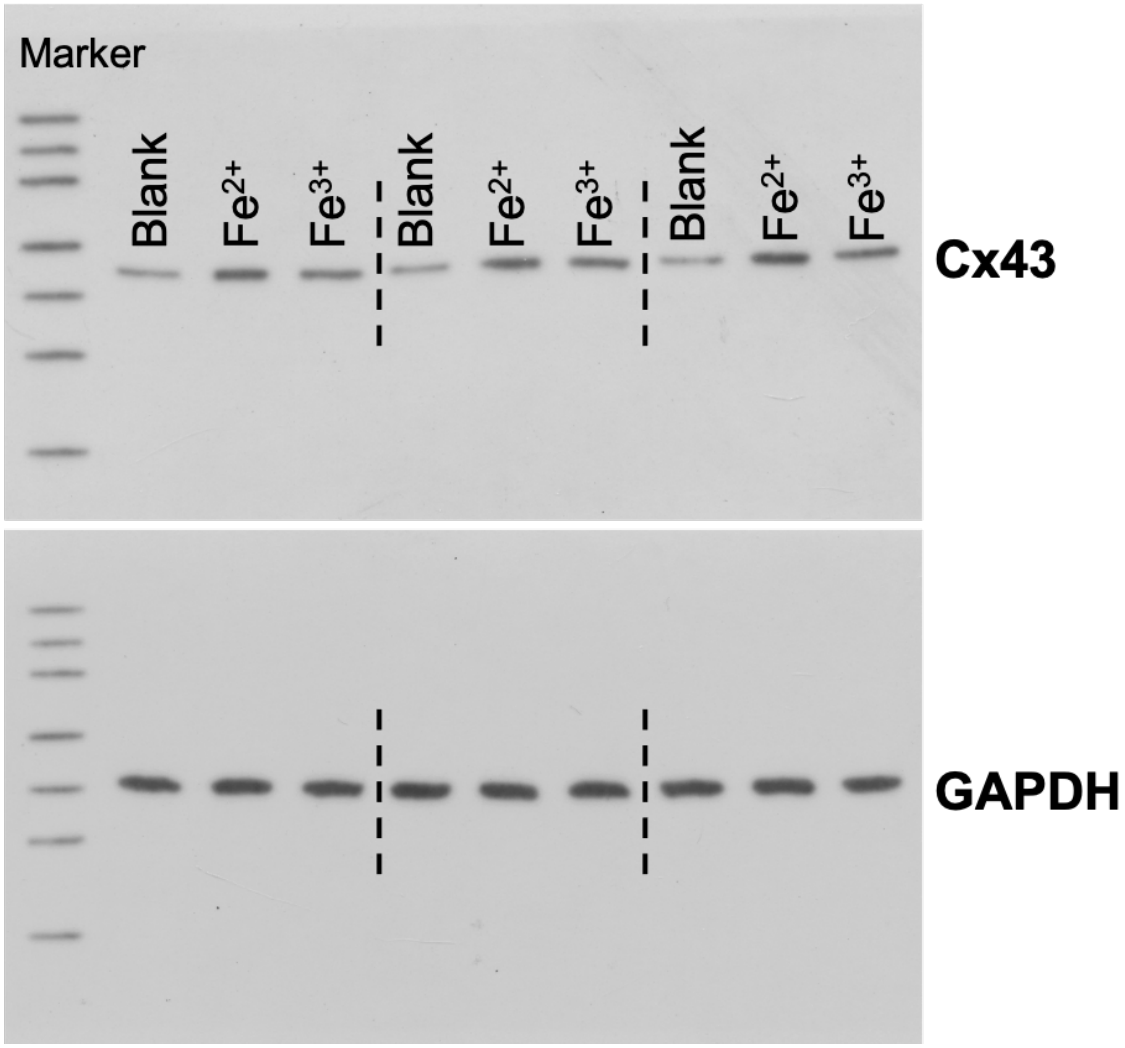

Fig. S3. The Cx43 expression of hMSCs post the treatment with $FeSO_4$ and $FeCl_3$. Western blot analysis was applied to compare the impacts of ferrous ions and ferric ions on the Cx43 expressions in hMSCs. hMSCs without iron treatment was as the blank group. Each group was repeated for thrice. (n = 3).

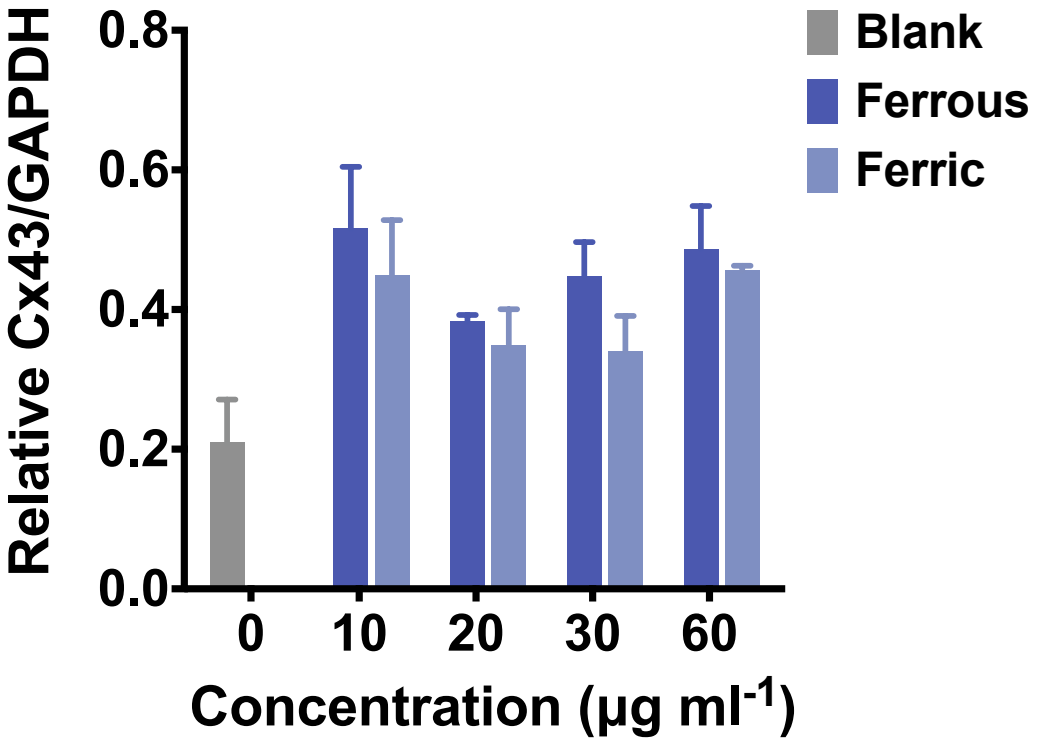

Fig. S4. Cx43 expression in hMSCs after treatment with free iron ions at different concentrations. Semiquantitative results of the Cx43 expression levels in hMSCs after treating with ferrous sulfate and ferric trichloride at different concentrations according to the Western blot analysis. (n = 3). Data are presented as means ± SD.

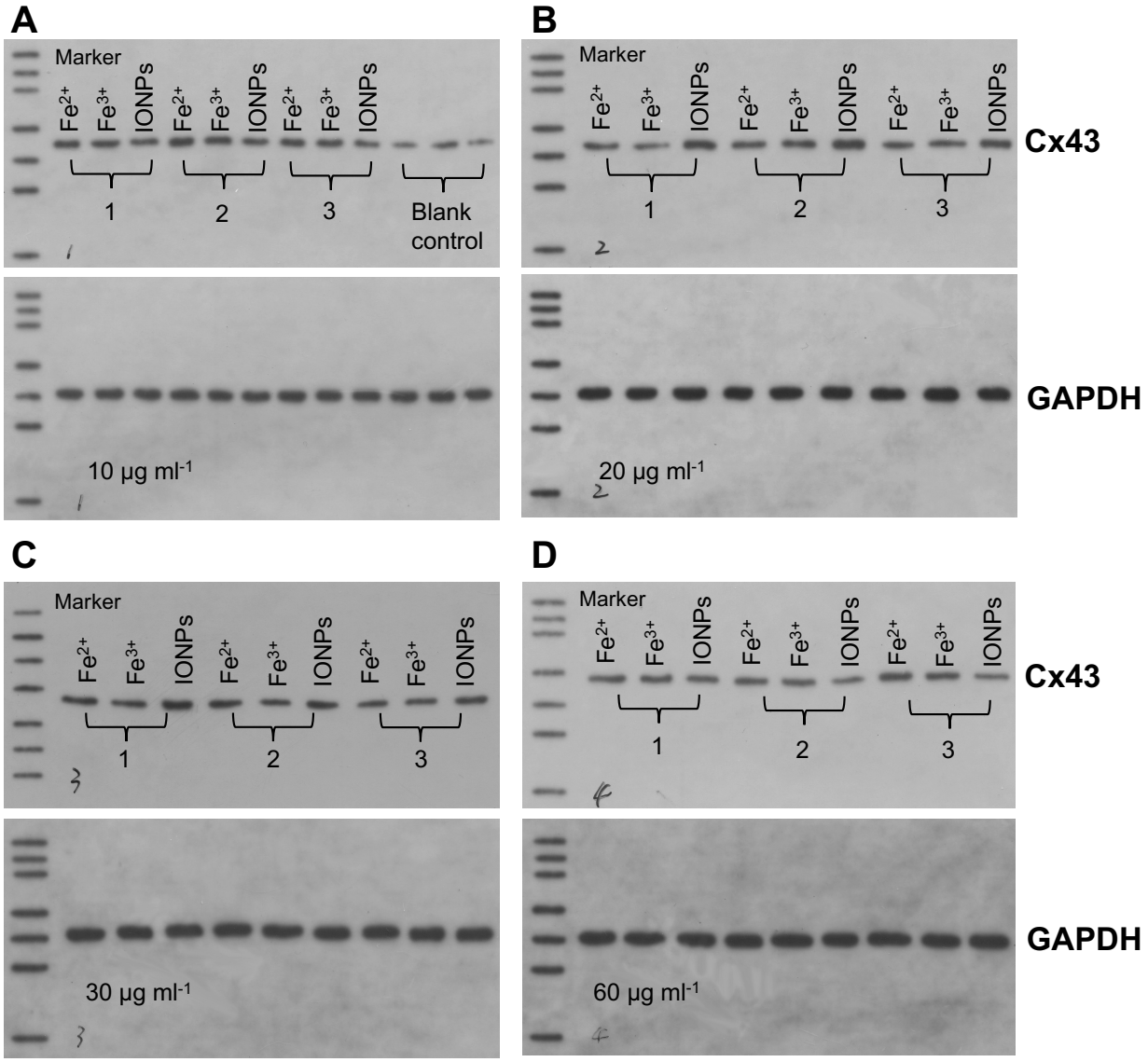

Fig. S5. Levels of Cx43 expression in hMSCs triggered by iron ions and IONPs at different concentrations. Western blot analysis was applied to evaluate the Cx43 expressions in hMSCs after the incubation with ferrous sulfate solution, ferric trichloride solution or IONPs for 24 h at different concentrations. Each group was repeated for thrice.(n = 3).

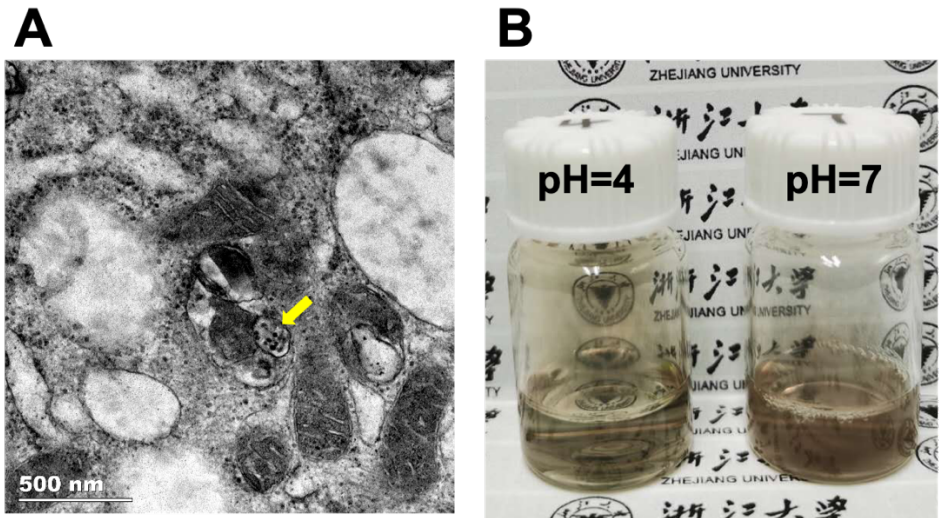

Fig. S6. Intracellular distribution and degradation of IONPs at low pH. (A) Transmission electron microscopy (TEM) image demonstrated the endocytosed IONPs mainly existed in lysosomes (indicated by yellow arrow). Scale bar, 500 nm. **(B)** Images of IONPs (30 μg ml^{-1}) after 24 h incubation in pH 4 or pH 7 solution. Photo Credit: Tianyuan Zhang and Huang Ting, Zhejiang University.

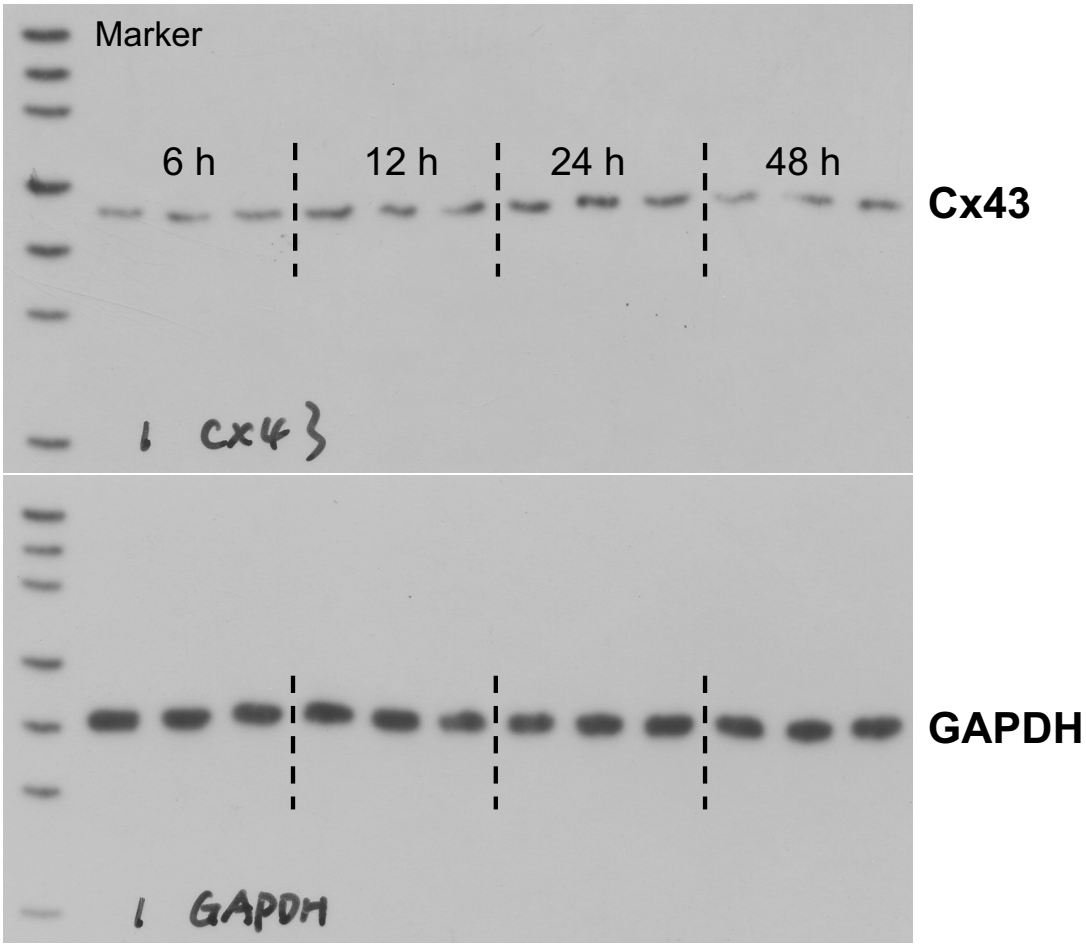

Fig. S7. The Cx43 expression of hMSCs at indicated time points. Western blot analysis was applied to evaluate the Cx43 expressions of hMSCs after the cellular uptake of IONPs at various time points. Each group was repeated for thrice. (n = 3).

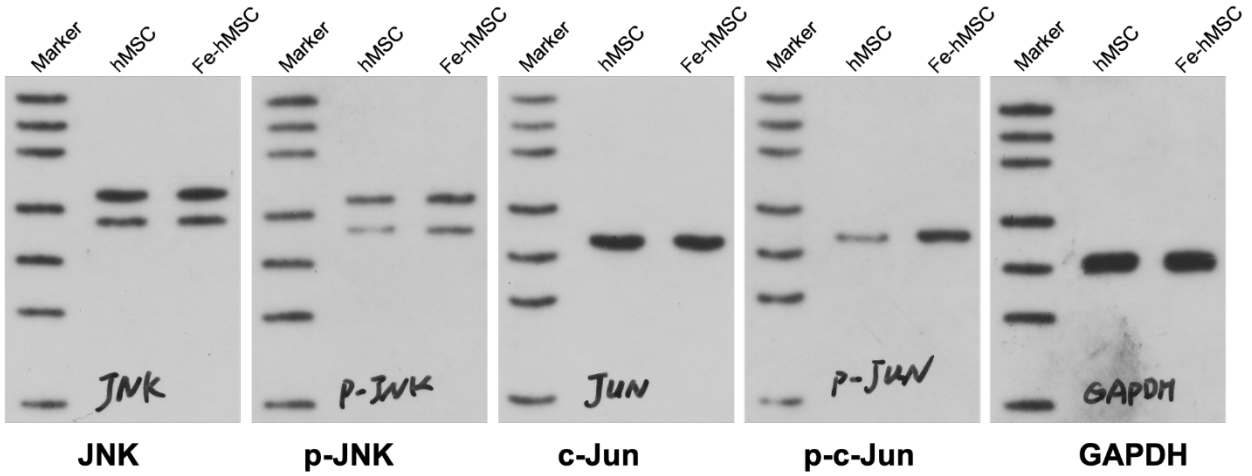

Fig. S8. Original images for the upregulation of JNK pathway triggered by IONPs. The intracellular signalling cascades of JNK pathway of hMSC and Fe-hMSC were assessed by Western blot analysis.

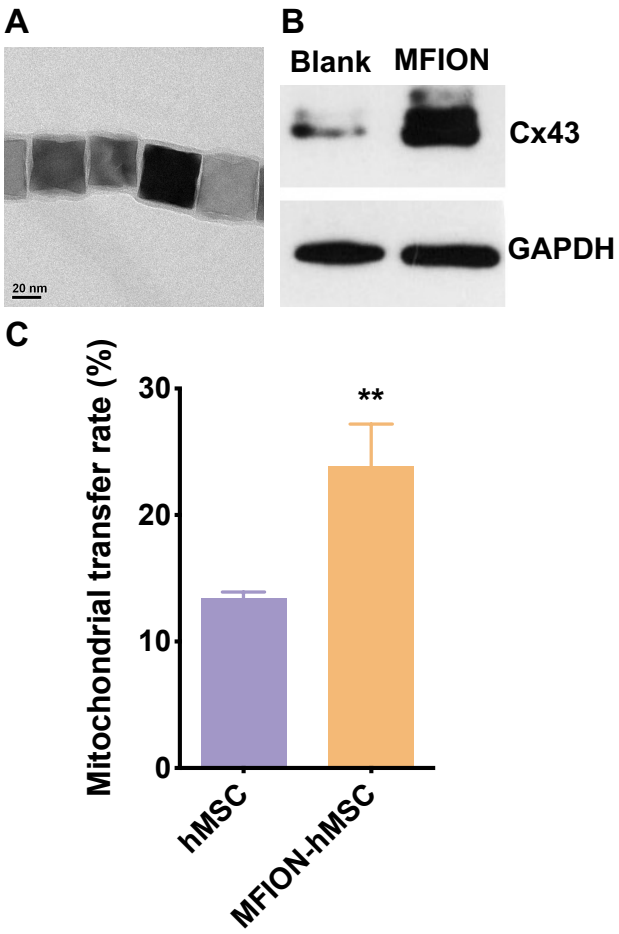

Fig. S9. The ferrimagnetic iron oxide nanocubes (MFION) could trigger the overexpression of Cx43 and promote the mitochondrial transfer of hMSC. (A) TEM of MFION showed the uniform nanocubes with the size about 22 nm. Scale bar, 20 nm. **(B)** Cx43 expression in hMSC was assessed by Western blot analysis at 24 h post the cellular uptake of MFION (10 μg ml^{-1}). **(C)** Mitochondrial transfer ability of hMSC and MFION-engineered hMSC (MFION-hMSC) toward bleomycin treated TC-1 cells (BLM-TC-1 cells) (n = 3). Data are presented as means ± SD. Statistical significance was calculated via unpaired Student's t test. $^{**}P < 0.01$.

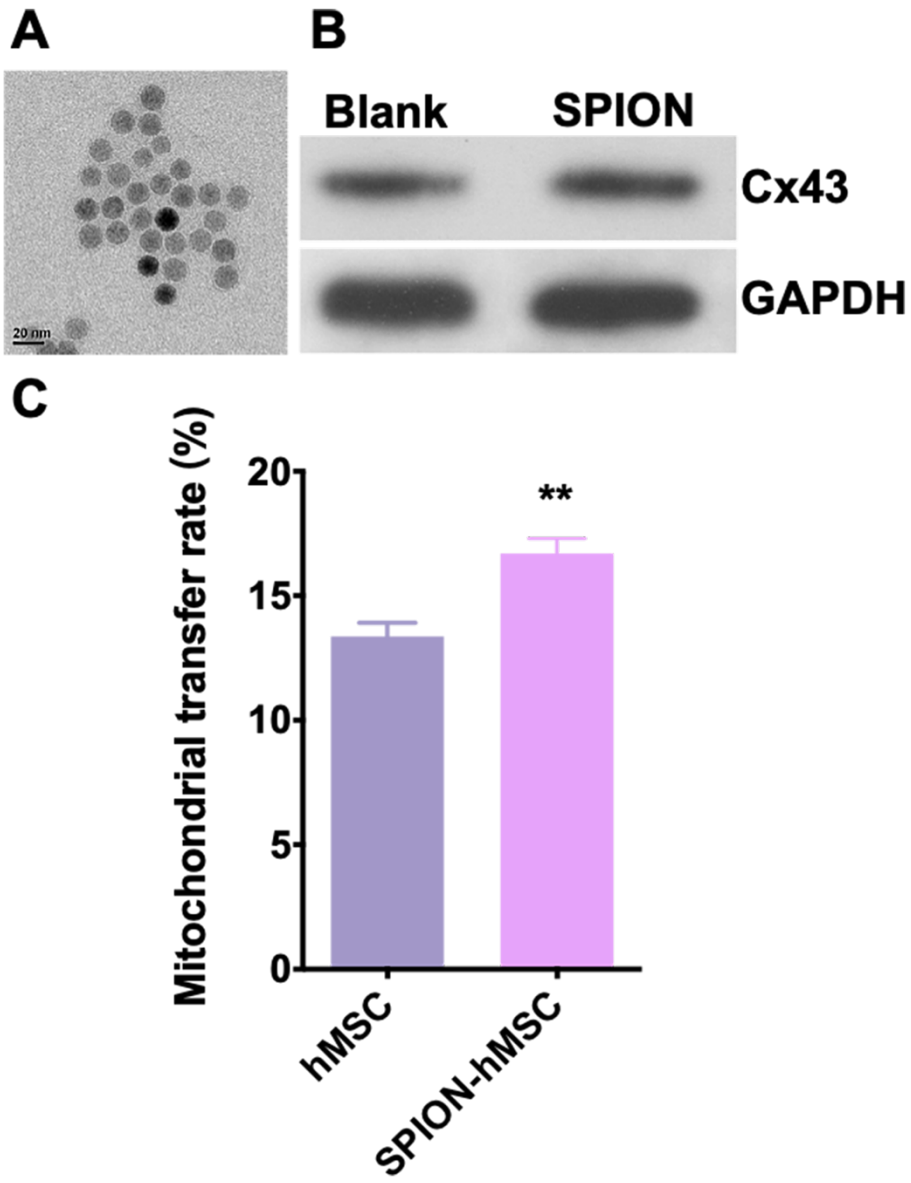

Fig. S10. The commercial superparamagnetic iron oxide nanoparticles (SPIONs) produced by Aladdin Co. Ltd. (U196711) triggered the overexpression of Cx43 and promoted the mitochondrial transfer of hMSC. (A) TEM of the commercially available SPIONs. Scale bar, 20 nm. **(B)** Cx43 expression in hMSCs was assessed by Western blot analysis at 24 h post the cellular uptake of SPIONs (30 μg ml^{-1}). **(C)** Mitochondrial transfer ability of hMSCs and SPION-hMSCs toward BLM-TC-1 cells (n = 3). Data are presented as means ± SD. Statistical significance was calculated via unpaired Student's t test. $^{**}P < 0.01$.

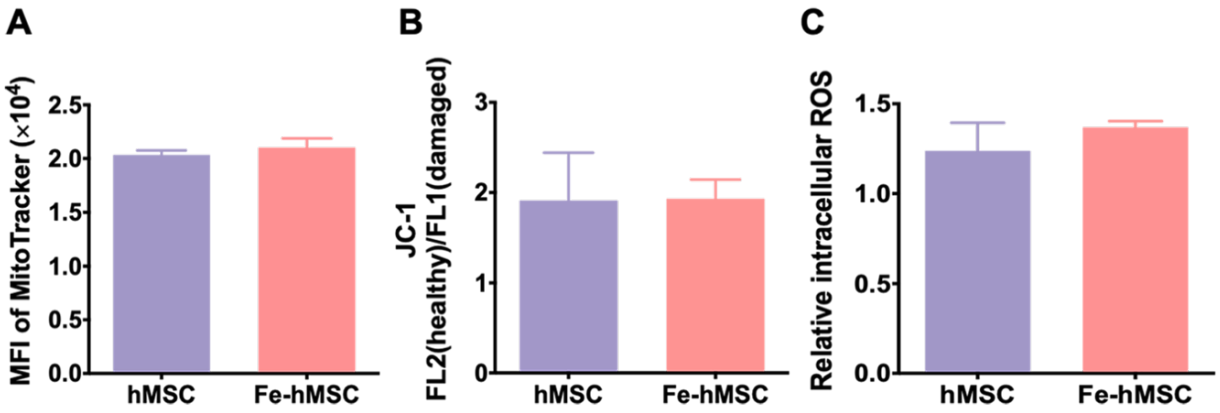

Fig. S11. Impacts of the cellular uptake of IONPs (30 μg ml^{-1}) on the mitochondrial amount and mitochondrial function of hMSC. (A) The mean fluorescent intensity (MFI) of labelled mitochondria determined via flow cytometry analysis (n = 3). **(B)** The mitochondrial membrane potentials were indicated by using JC-1 mitochondrial membrane potential kit (n = 3). **(C)** The relative intracellular reactive oxygen species (ROS) levels were analyzed via flow cytometry (n = 3). No significant difference between groups was observed. Data are presented as means ± SD. Statistical significance was calculated via unpaired Student's t test.

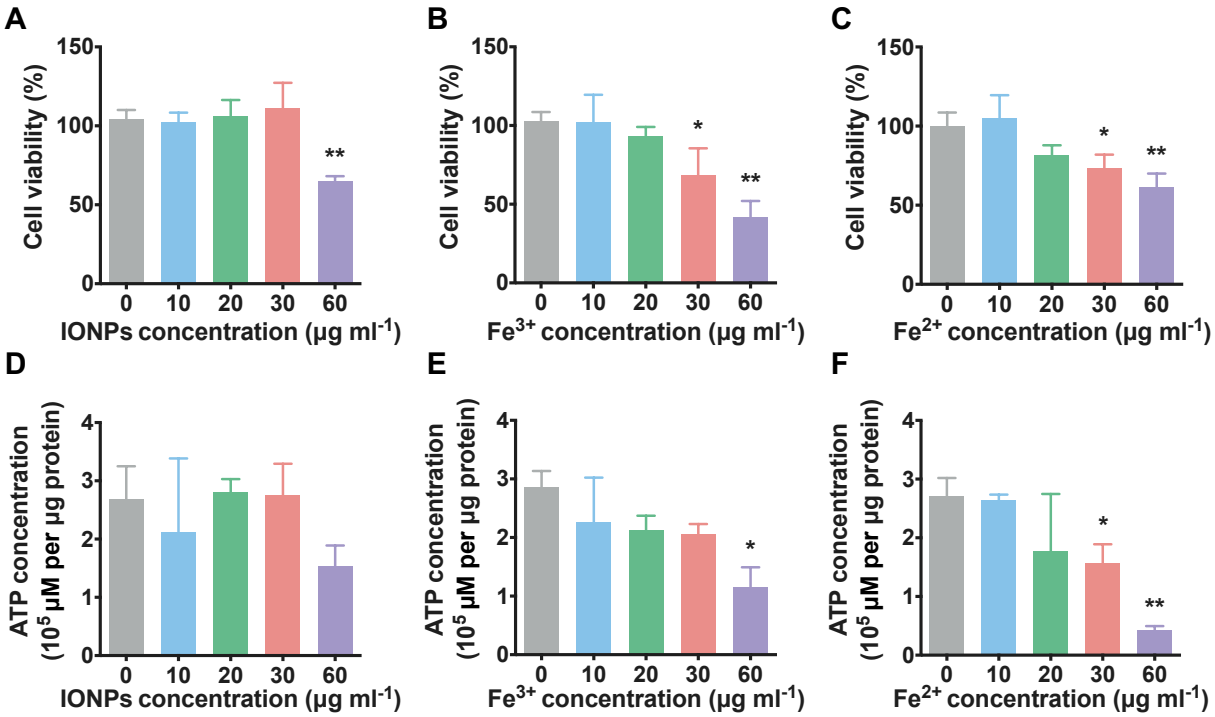

Fig. S12. Comparisons of the impacts caused by IONPs and free iron ions treatments on the cell viability and intracellular ATP levels of hMSCs. (A) Cell viability of hMSCs after treating with IONPs at the indicated iron concentrations (n = 3). **(B)** Cell viability of hMSCs after treating with ferric chloride solutions at the indicated iron concentrations (n = 3). **(C)** Cell viability of hMSCs after treating with iron sulfate solution at the indicated iron concentrations (n = 3). **(D)** Intracellular ATP levels in hMSCs after treating with IONPs at the indicated iron concentrations (n = 3). **(E)** Intracellular ATP levels in hMSCs after treating with ferric chloride solution at the indicated iron concentrations (n = 3). **(F)** Intracellular ATP levels in hMSCs after treating with iron sulfate solution at the indicated iron concentrations (n = 3). Data are presented as means ± SD. Statistical significance was calculated via ordinary one-way ANOVA. $^{**}P < 0.01$, $^{*}P < 0.05$.

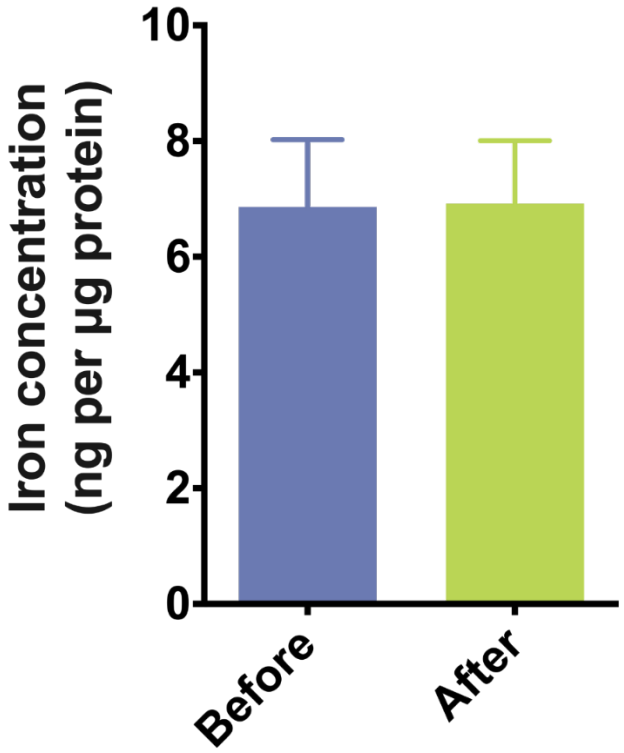

Fig. S13. Comparison of iron concentration in TC-1 cells before and after co-culturing with Fe-hMSC. Green fluorescent protein expressed TC-1 cells were cocultured with Fe-hMSC for 24 h, the iron concentration in these cocultured TC-1 cells was then determined and compared to the iron concentration in TC-1 cells before the coculture (n = 4). Data are presented as means ± SD.

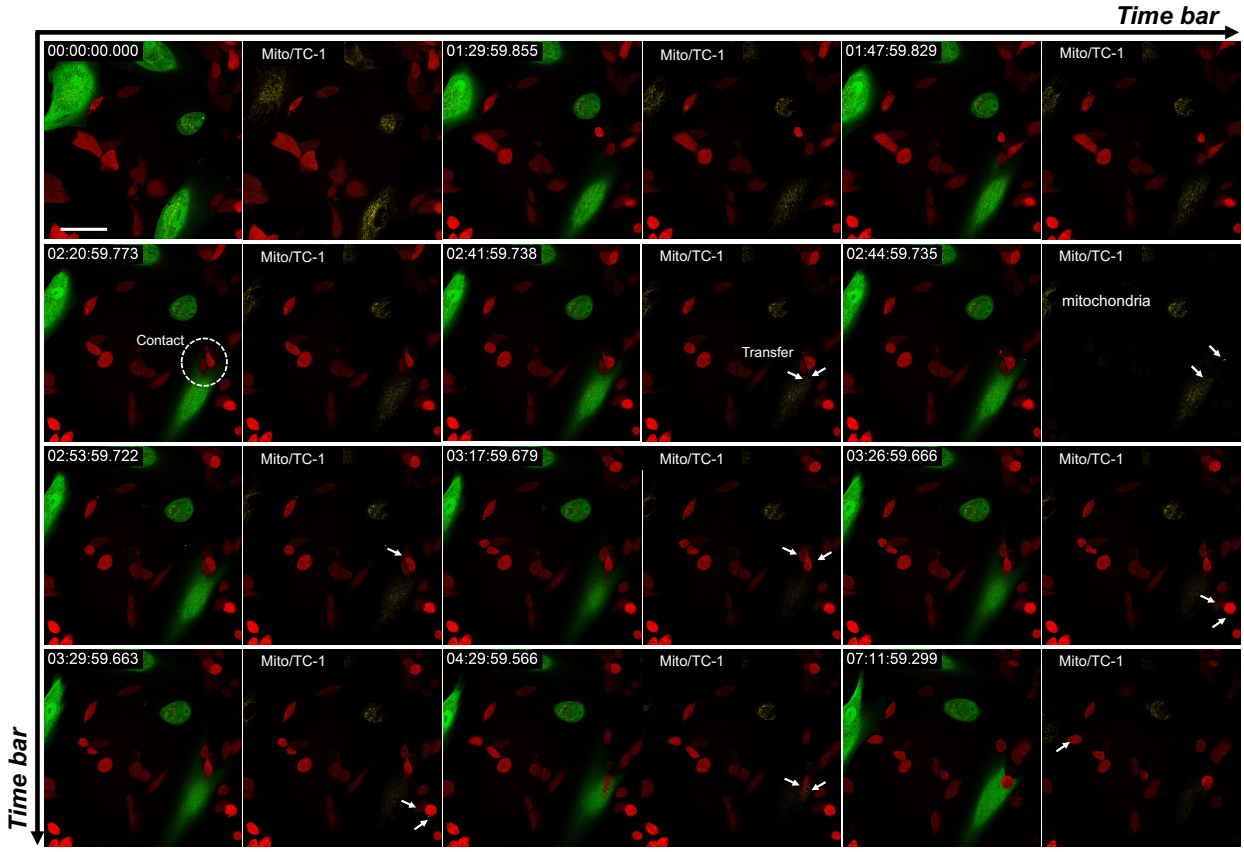

Fig. S14. Images of the continuously monitoring of the intercellular transfer of mitochondrial from Fe-hMSCs to BLM-TC-1 cells. The dynamics of mitochondrial transfer were monitored by confocal laser scanning microscopy over 8 h. An obvious intercellular transfer of mitochondria toward BLM-TC-1 cells was found at about 2 h 40 min post the coculture. Green: Green fluorescent protein expressed Fe-hMSCs (GFP-Fe-hMSCs), red: BLM-TC-1 cells, yellow: mitochondria of GFP-Fe-hMSCs. The white cycle indicates the cell-to-cell contact, and white arrows indicate the mitochondrial transfer. Scale bar, 25 μm.

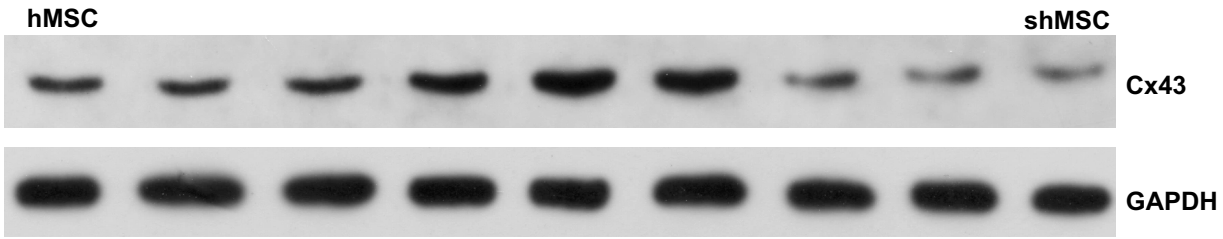

Fig. S15. Cx43 expression of shMSC after the gene transfection using Cx43-siRNA. An obvious downregulation of Cx43 expression levels of transfected shMSCs was observed by using Western blot analysis.

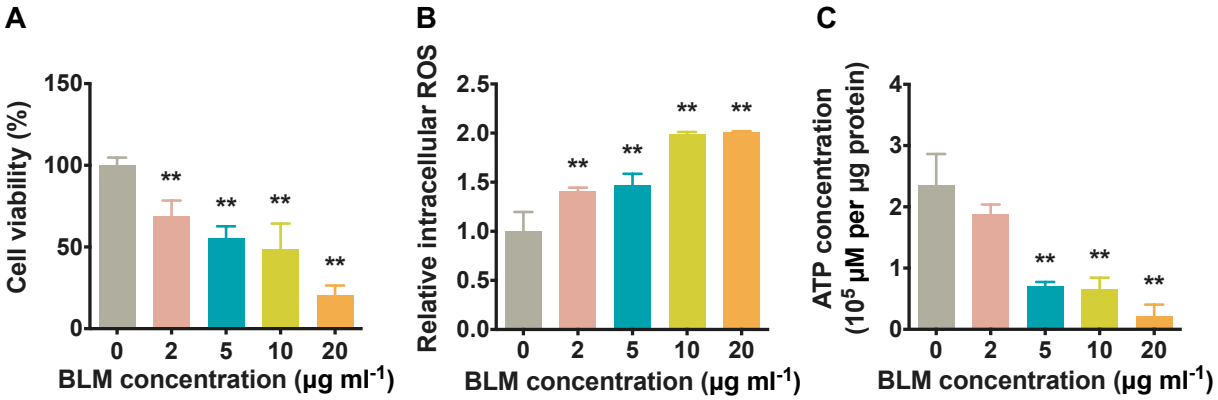

Fig. S16. Cell injury degrees induced by the treatment with bleomycin (BLM) at different concentrations (A) Cell viability of TC-1 cells after treatment with BLM at the indicated concentrations for 24 h (n = 3). **(B)** Relative intracellular ROS levels of TC-1 cells after treatment with BLM at the indicated concentrations for 24 h (n = 3). **(C)** Intracellular ATP levels of TC-1 cells after treatment with BLM at the indicated concentrations for 24 h (n = 3). Data are presented as means ± SD. Statistical significance was calculated via ordinary one-way ANOVA. $^{**}P < 0.01$.

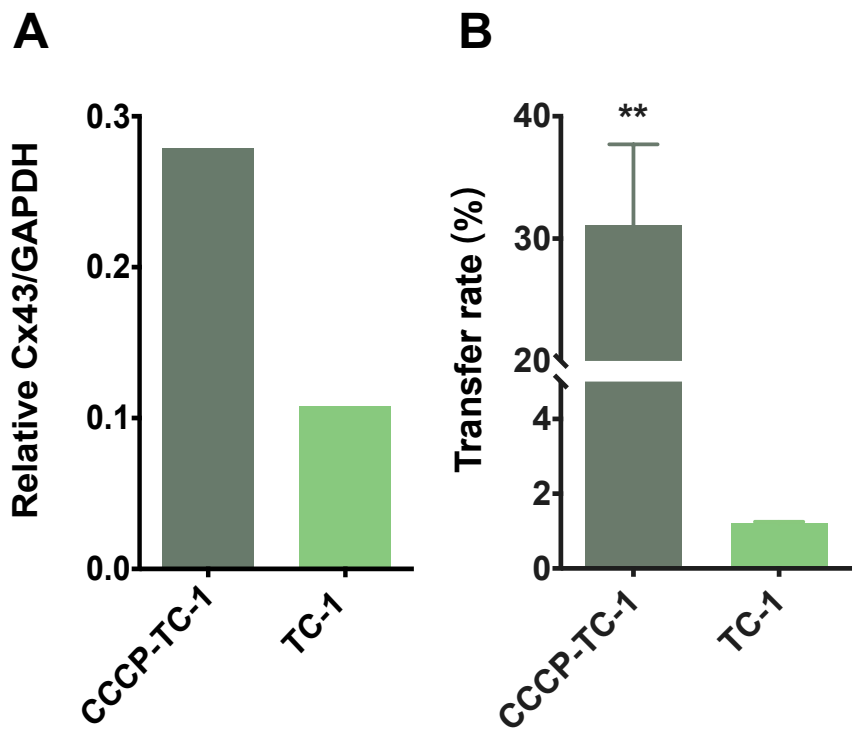

Fig. S17. Cx43 expression and mitochondrial transfer rate of TC-1 cells post the treatment of carbonyl cyanide 3-chlorophenylhydrazone (CCCP). (A) Semiquantitative data of the Cx43 expression levels in TC-1 cells and TC-1 cells treated with CCCP (CCCP-TC-1) assessed by Western blot analysis. **(B)** Quantitative comparison of mitochondrial transfer rates from Fe-hMSC toward CCCP-TC-1 cells after a 24 h coculture (n = 3). Statistical significance was calculated via unpaired Student's t- test. $^{**}P < 0.01$.

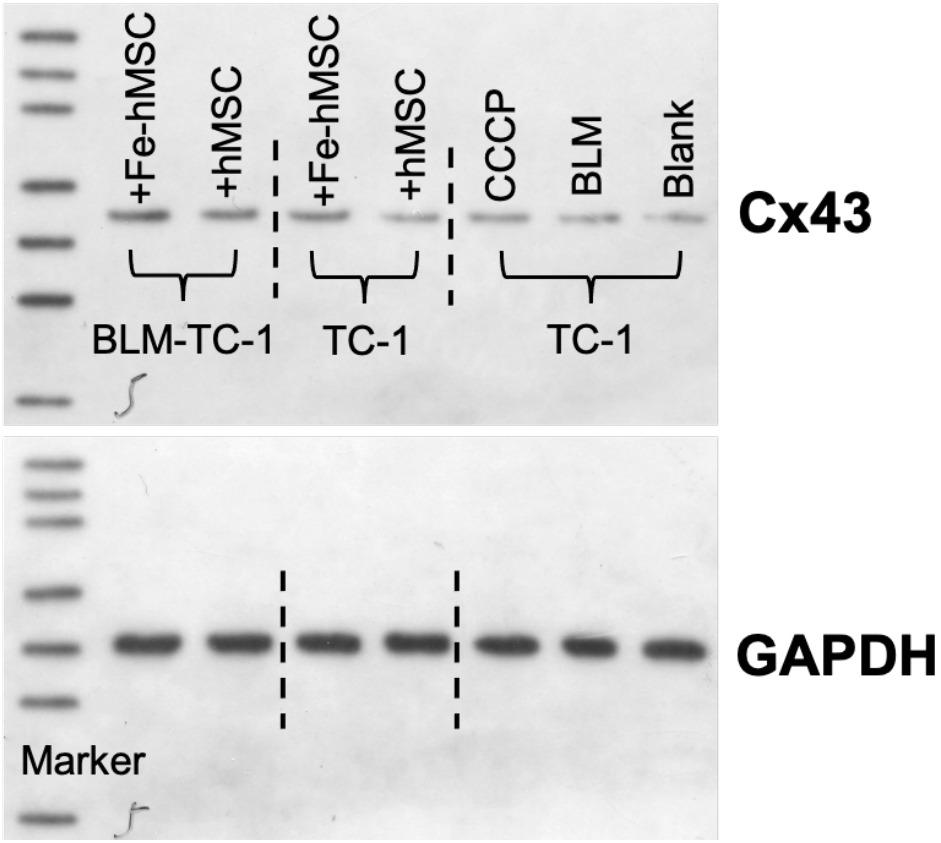

Fig. S18. Levels of Cx43 expression in TC-1 cells after the indicated treatments. Western blot analysis was applied to determine the Cx43 expression in TC-1 cells.

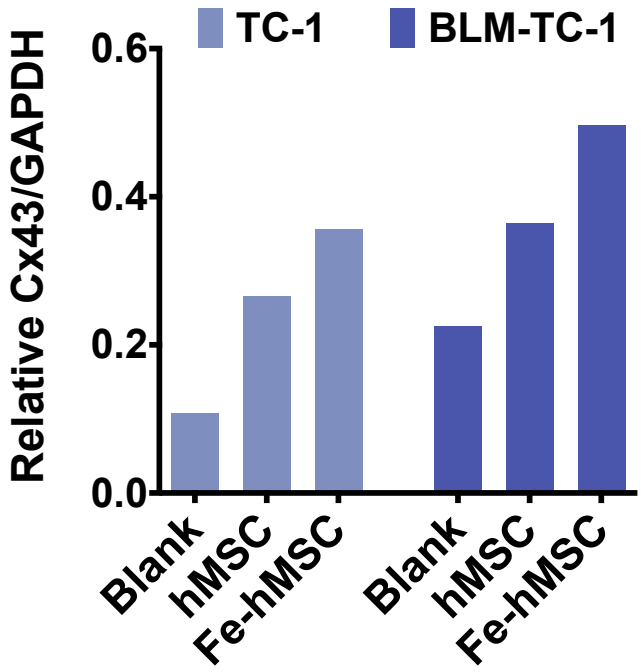

Fig. S19. Semiquantitative results of the Cx43 expression levels in TC-1 cells and BLM treated TC-1 cells (BLM-TC-1 cells) after coculture with hMSC and Fe-hMSC. Healthy TC-1 cells and BLM-TC-1 cells were cocultured with hMSC or Fe-hMSC for 24 h, followed by their isolation to determine the Cx43 expression levels via Western blot analysis.

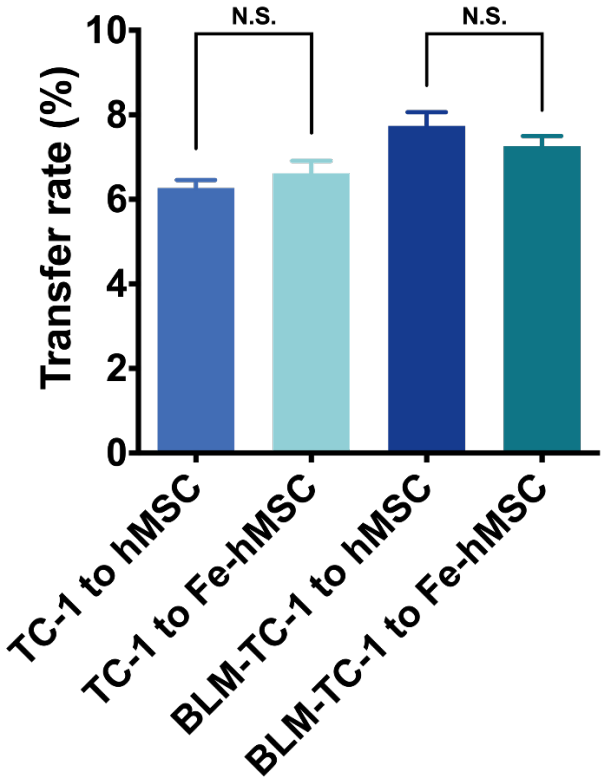

Fig. S20. The intercellular transfer rate of mitochondria between TC-1 cells and hMSC. Flow cytometry analysis was applied to assess the mitochondrial transfer rate post 24 h coincubation (*n* = 3). Data are presented as means ± SD. Statistical significance was calculated via ordinary one-way ANOVA.

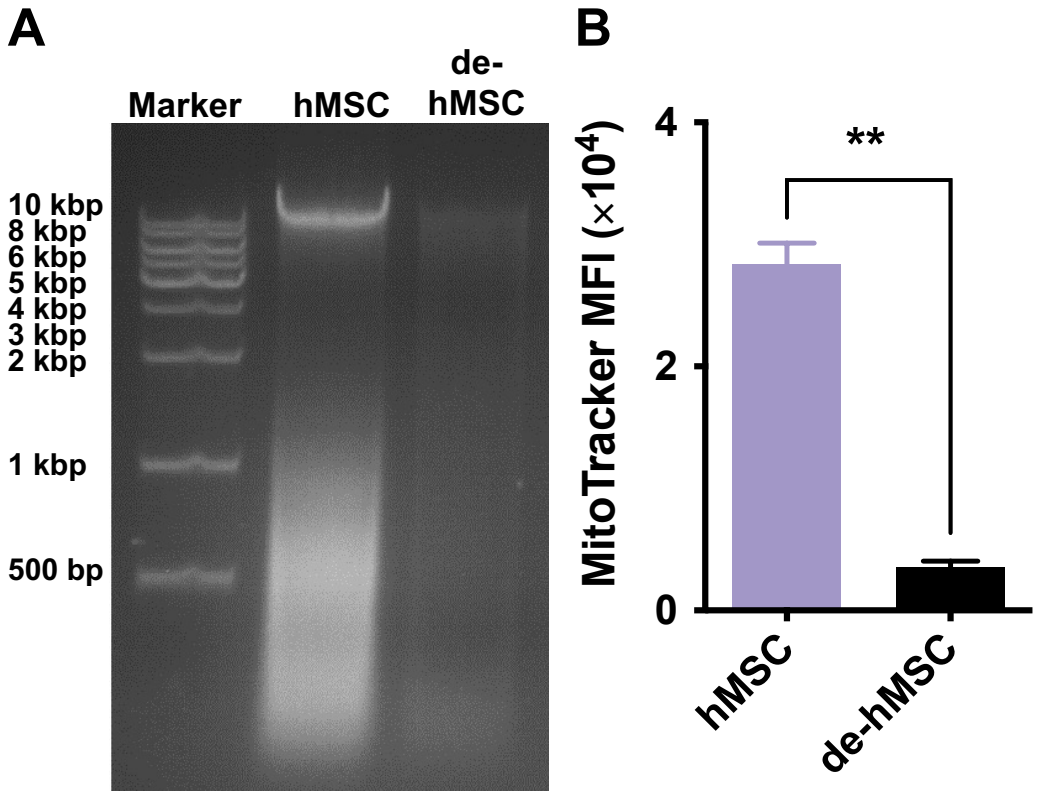

Fig. S21. Confirmation of mitochondrial DNA (mtDNA) depleted hMSC (de-hMSC). (A) mtDNA in hMSCs and de-hMSCs was assessed via polymerase chain reaction agarose gel analysis. **(B)** Quantitative evaluation of the mitochondrial mass in hMSCs and de-hMSCs via the measurement of mean fluorescence intensity (MFI) of MitoTracker-labeled mitochondria ($n = 3$). Data are presented as means ± SD. Statistical significance was calculated via unpaired Student's t test. $^{**}P < 0.01$.

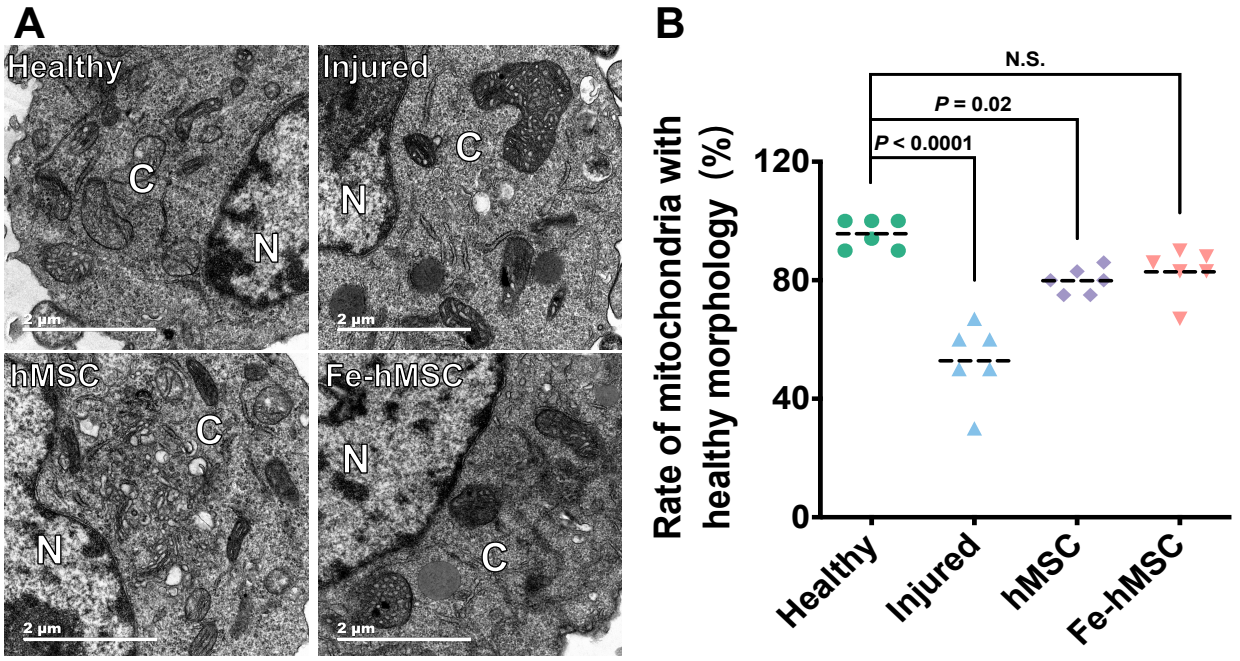

Fig. S22. Mitochondria with healthy morphology in TC-1 cells were observed and quantitively calculated. (A) TEM images of the mitochondria in healthy TC-1 cells and BLM-TC-1 cells after indicated treatments. N refers to the cell nucleus and C refers to the cytoplasm. Scale bars, 2 μm **(B)** The ratio of mitochondria with healthy morphology in TC-1 cells ($n = 6$). Data are presented as means ± SD. Statistical significance was calculated via ordinary one-way ANOVA.

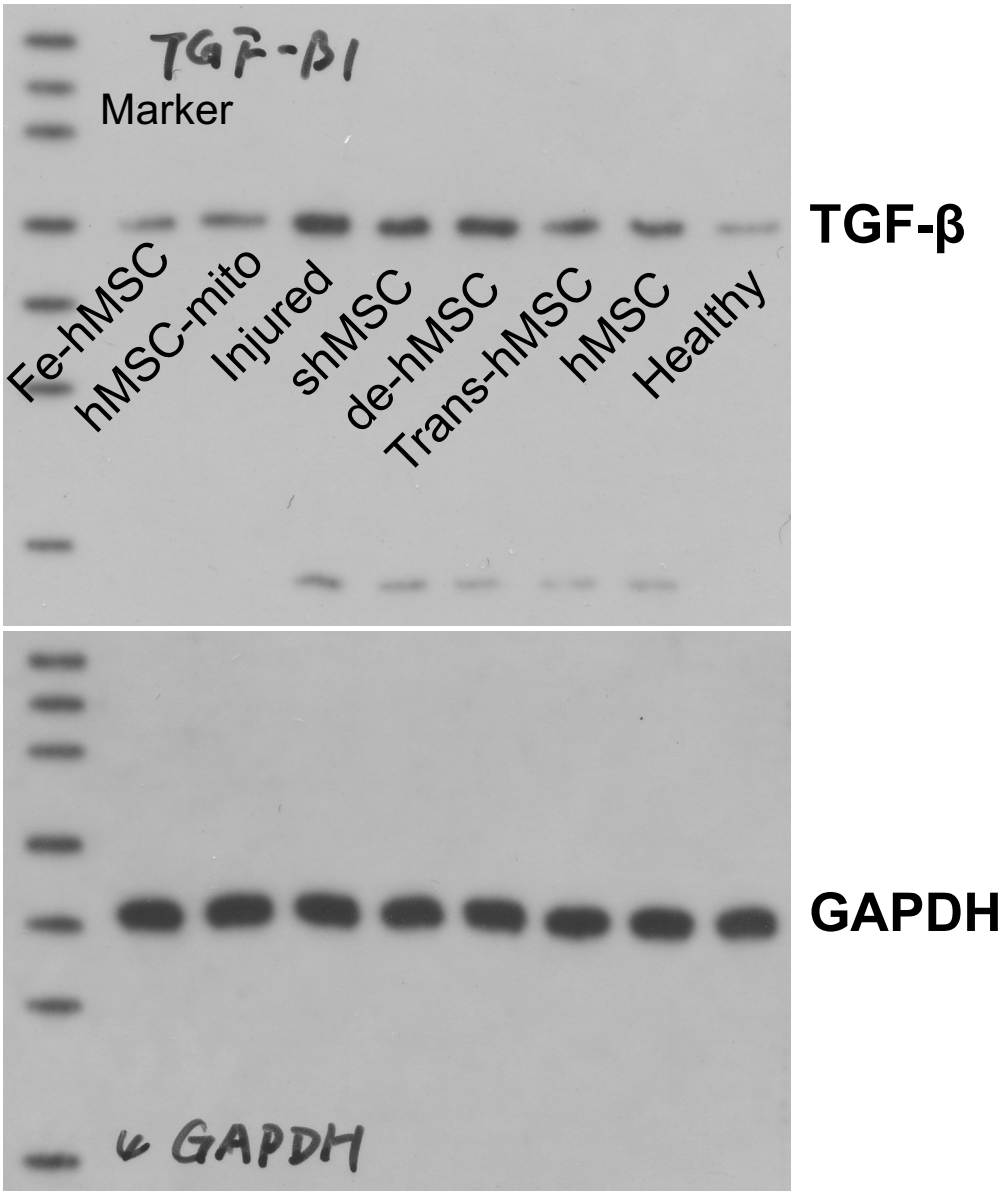

Fig. S23. Transforming growth factor-β (TGF-β) expression of healthy TC-1 cells and BLM-TC-1 cells after various treatments. Western blot analysis was applied to evaluate the TGF-β expression levels.

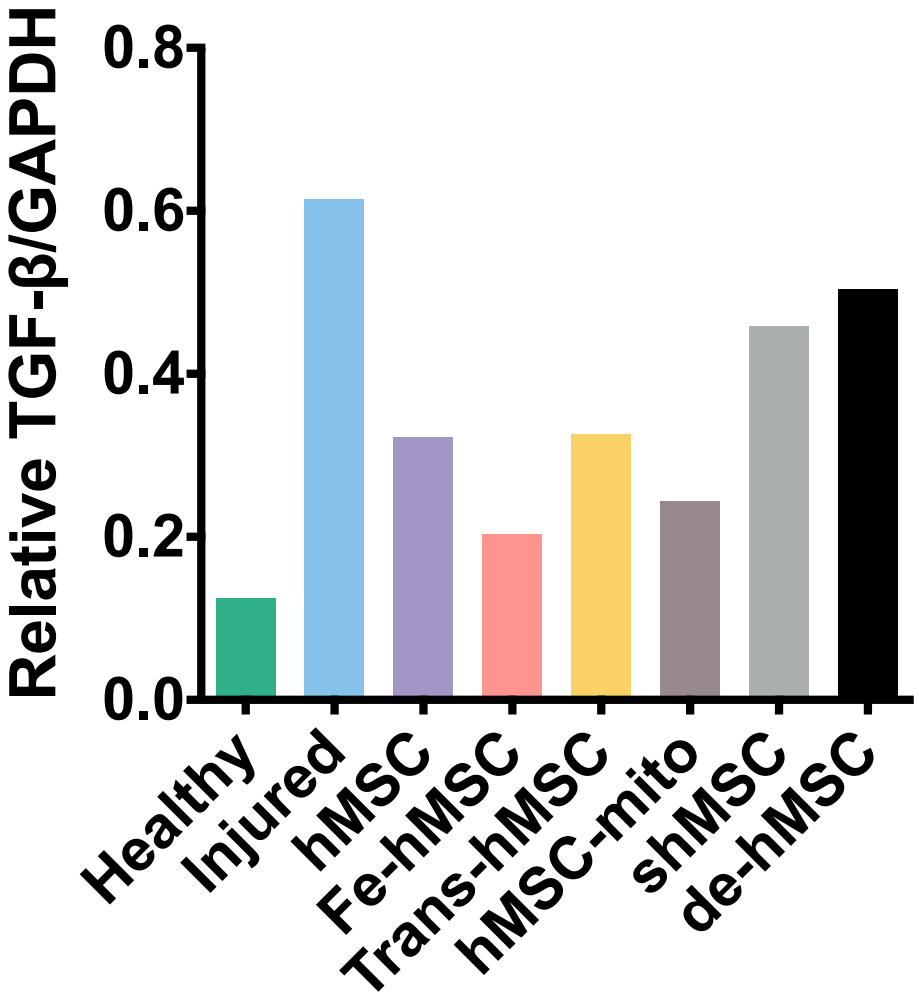

Fig. S24. Semiquantitative data of TGF-β expression according to the above Western blot analysis (Fig. S23). TGF-β expression levels were semiquantified with the normalization of GAPDH levels.

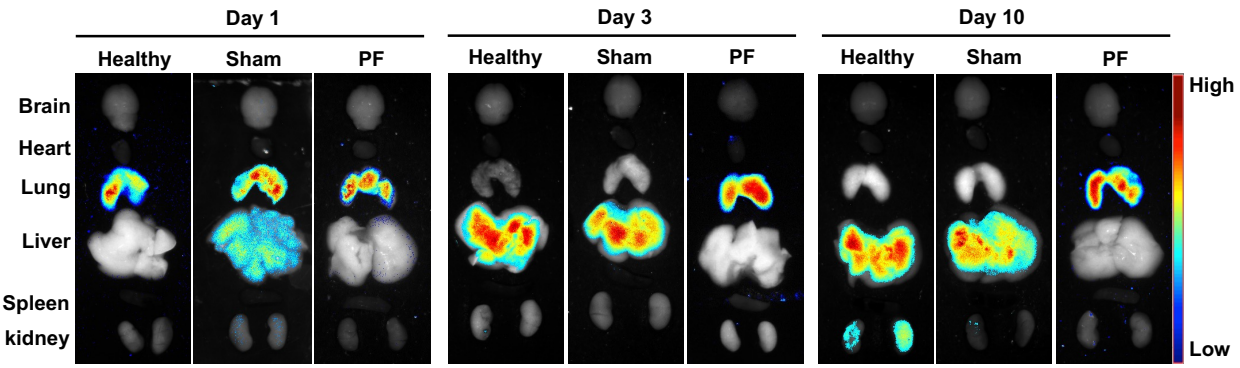

Fig. S25. The biodistribution of Fe-hMSCs post systemic administration through tail vein. Fe-hMSCs were observed mainly distributed in lungs. In addition, Fe-hMSCs showed a significantly prolonged retention in fibrotic lungs. PF: pulmonary fibrosis.

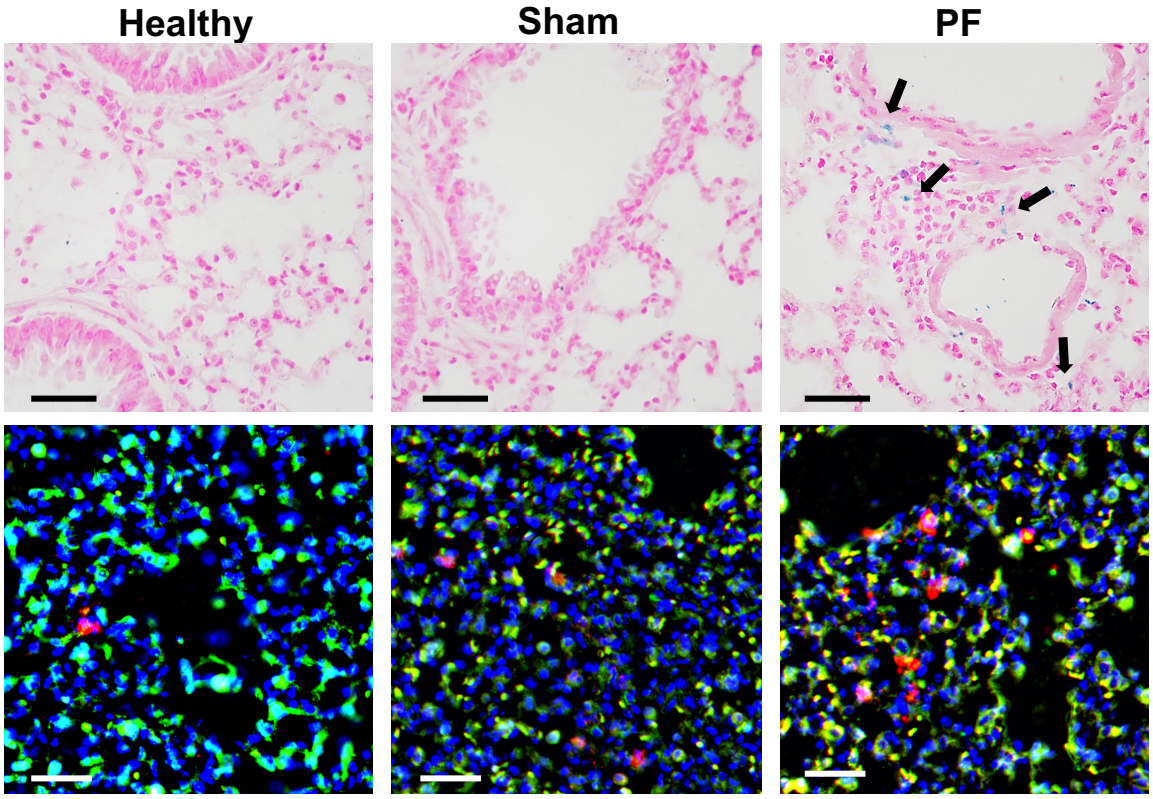

Fig. S26. Microscopy examinations of the lung sections on 10 days post the initial administration. The upper panel is the images after Prussian blue staining, where obvious signals of iron (black arrows) can be observed in fibrotic lung, indicating the lung homing of Fe-hMSC. The bottom panel is the images after immunofluorescent staining, in which a much higher number of Fe-hMSCs is observed in fibrotic lung. In addition, the cell-to-cell contract between Fe-hMSC and alveolar epithelial cell (AEC) was observed (blue: nuclei, green: AECs, red: Fe-hMSCs). Scale bars, 50 μm for the upper panel and 40 μm for the bottom panel.

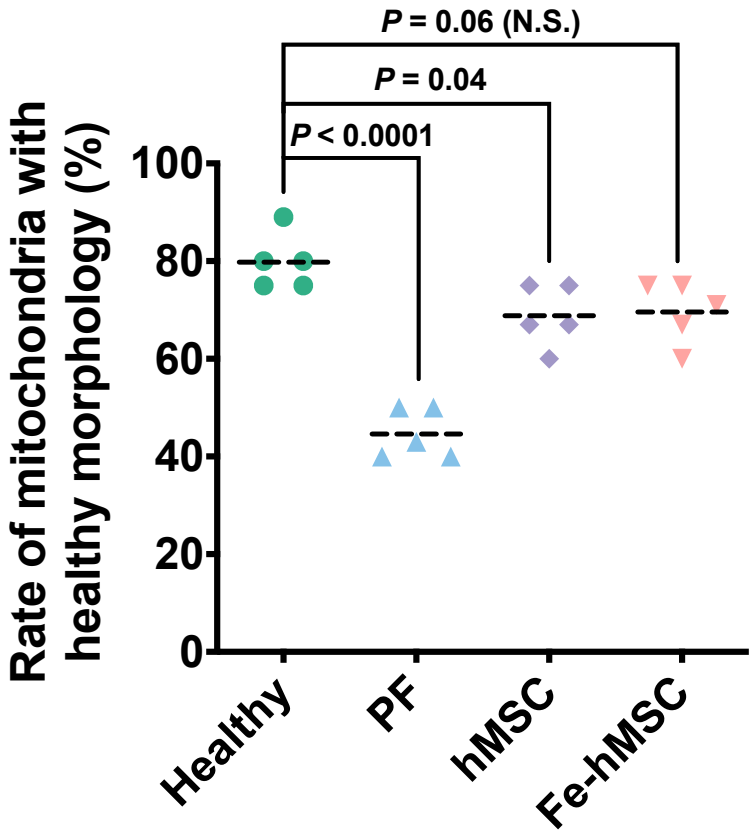

Fig. S27. Quantitative evaluation of the ratio of mitochondria with healthy morphology in AECs. The mitochondria with healthy morphology were counted according to the TEM images in Fig. 5G (n = 5). Data are presented as means ± SD. Statistical significance was calculated via ordinary one-way ANOVA.

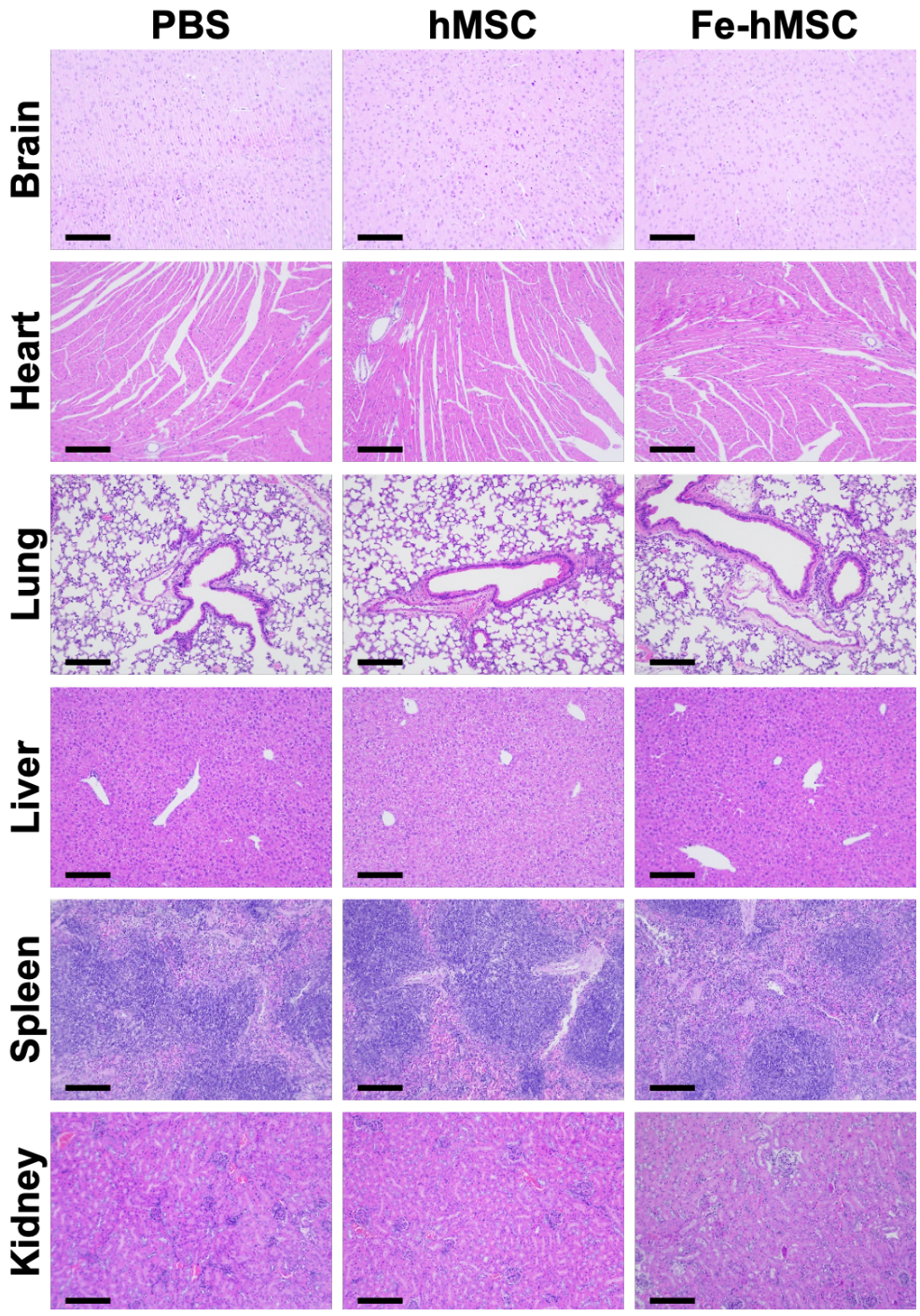

Fig. S28. Pathological examination of major organs in C57BL/6 mice through H&E staining. No significant detrimental effects were observed post the treatment of hMSC or Fe-hMSC. Scale bars, 200 μm.

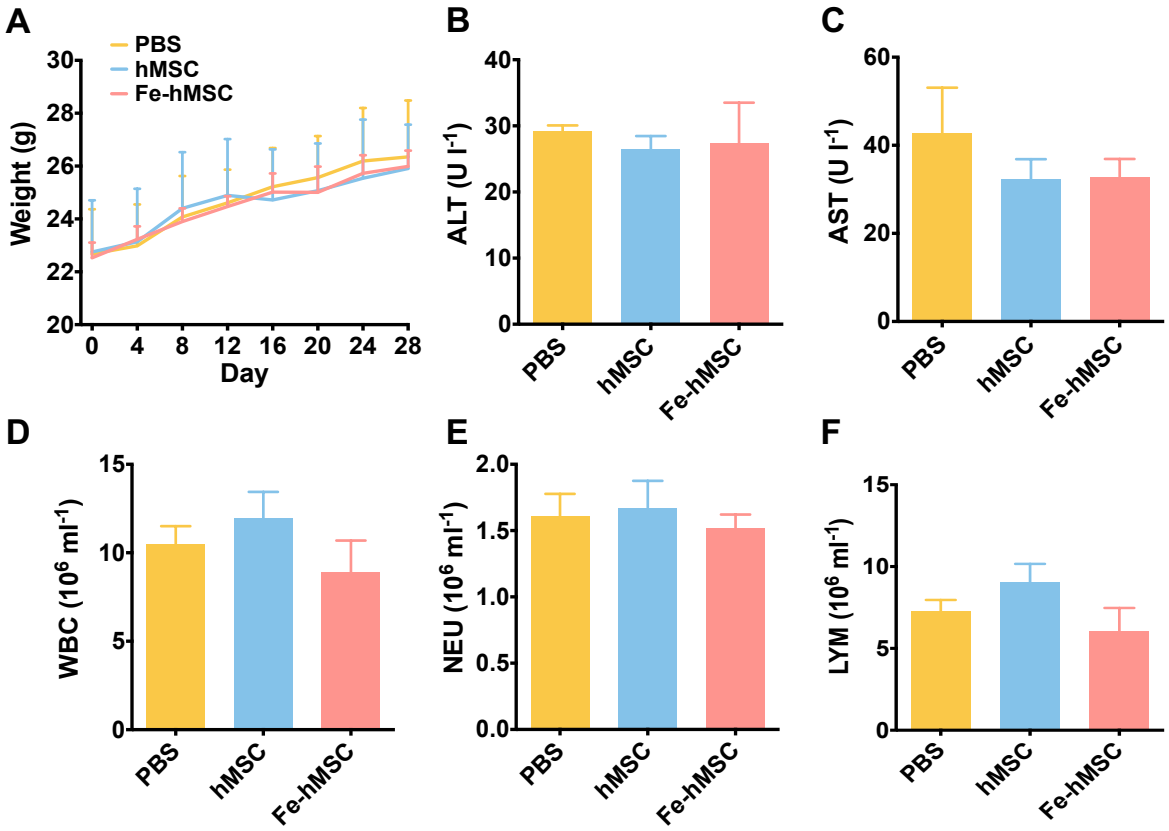

Fig. S29. Preliminary safety evaluations for the treatment using Fe-hMSC. (A) Body weight of C57BL/6 mice post the indicated treatments (n = 3). **(B)-(F)** Alanine transaminase (ALT), aspartate transaminase (AST), white blood cell (WBC), neutrophil (NEU), and lymphocyte (LYM) levels in mice blood (n = 3). Data are presented as means ± SD. Statistical significance was calculated via ordinary one-way ANOVA. No significant difference was observed compared with phosphate buffer saline (PBS) treatment group.

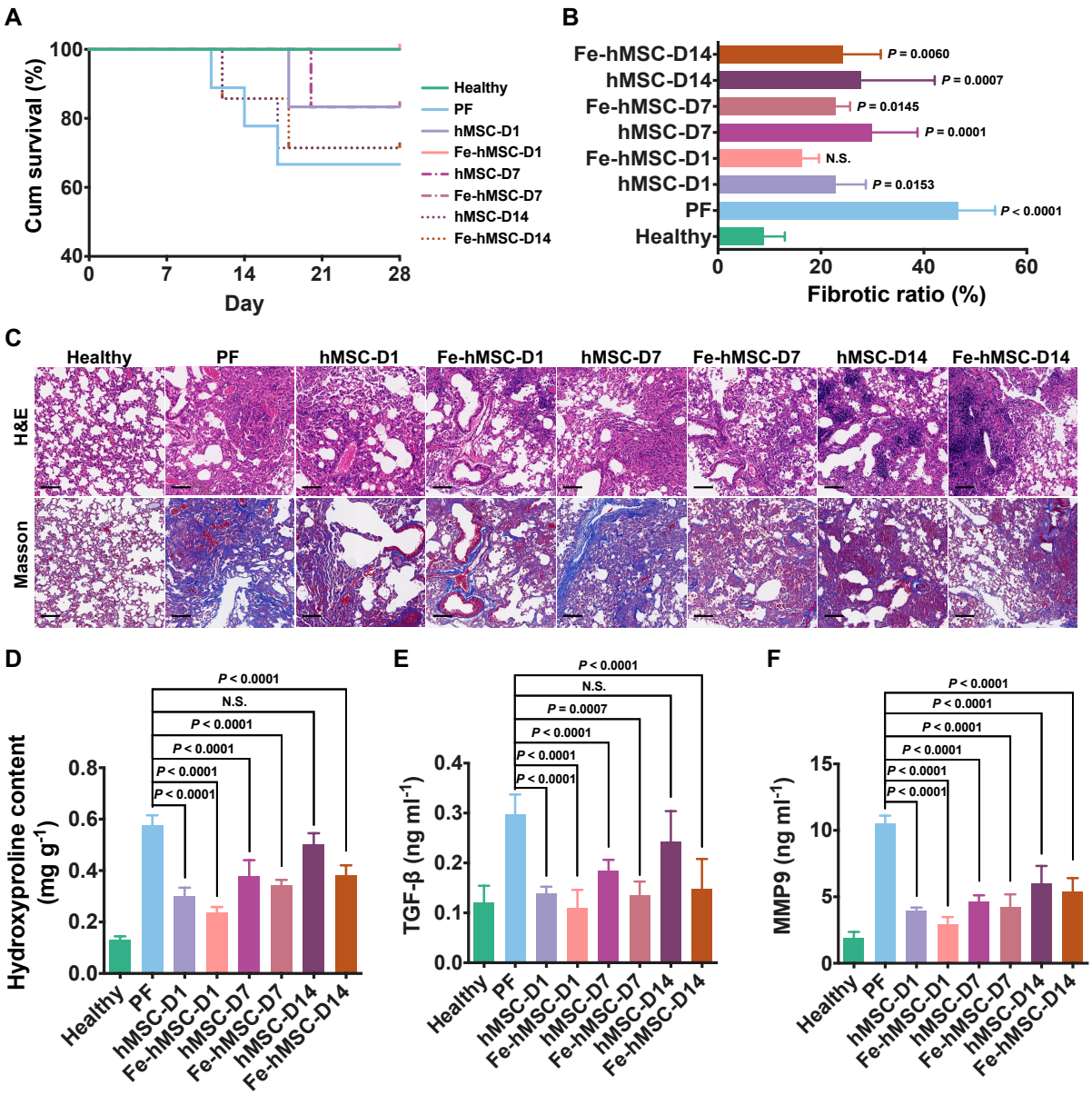

Fig. S30. Comparisons of the intervention efficiency against fibrotic progression in different progressed PF mice after the mitochondrial recharging treatment. Therapeutic hMSCs or Fe-hMSCs (5×10^5 cells per mouse) were systemically administered through the tail vein 1 day, 7 days and 14 days after BLM-induced injury. Curative evaluations were conducted on day 28 after BLM treatment. **(A)** Kaplan-Meier survival curves of fibrotic mice with various treatments (n = 6 for Healthy, hMSC-D1, Fe-hMSC-D1, hMSC-D7, Fe-hMSC-D7, n = 7 for hMSC-D7 and Fe-hMSC-D7, n = 9 for PF). **(B)** Quantitative data of the fibrotic area calculated from the pulmonary sections using Masson's trichrome staining via ImageJ (n = 5). **(C)** Representative images of the above Masson's trichrome staining and H&E staining of the pulmonary sections. Scale bars, 100 μm. **(D)** Levels of hydroxyproline in the lung homogenates (n = 5). **(E)** and **(F)** Amount of TGF-β and MMP9 in the bronchoalveolar lavage fluid (BALF) (n = 5). Data are presented as means ± SD (B, D-F). Statistical significance was calculated via Logrank test (A), and ordinary one-way ANOVA (B, D-F).

Supplementary Movies

Movie S1. The real-time monitoring of the mitochondrial transfer from Fe-hMSC toward BLM-TC-1 cells in a coculture system. Green: GFP-Fe-hMSCs, red: BLM-TC-1 cells, yellow: mitochondria of GFP-Fe-hMSCs. Scale bar: 25 μm.

Movie S2. The same movie of movie S1 but removed the fluorescent signals of GFP-Fe-hMSC for a better observation. Red: BLM-TC-1 cells, yellow: mitochondria of GFP-Fe-hMSCs. Scale bar: 25 μm.